Table I. ^{1}H and ^{13}C NMR data of methyl-3α,23-dihydroxy-17,14-friedolanstan-8,14,24-trien-26-oat isolated from *G. celebica* leaves.

	^{13}C NMR		^{1}H NMR	
No.	Chemical shift	Position	Chemical shift	Position
1	168.7	C-26		
2	148.9	C-14		
3	144.6	C-9		
4	142.6	C-24	6.72	H-24 (1H, *qd*, J=7.5 & 1.5 Hz)
5	127.3	C-25		
6	123.1	C-8		
7	116.0	C-15	5.26	H-15 (1H, *s*)
8	76.0	C-3	3.45	H-3 (1H, *br s*)
9	67.1	C-23	4.57	H-23 (1H, *ddd*, J=10.7, 7.5 & 2.5 Hz)
10	52.1	OMe	3.75	OMe (3H, *s*)
11	50.2	C-17		
12	48.2	C-13		
13	45.7	C-16	2.23-2.15 1.99-1.94	H-16, H-20 (2H, *m*) H-16 (1H, *m*)
14	44.6	C-5		
15	39.7	C-11		
16	38.0	C-10		
17	37.8	C-4		
18	33.6	C-20		
19	30.3	C-1	1.77-1.56	2x H-1, H2, H5, 2x H-6, 2x H-12, H-11 (9H, *m*)
20	29.4	C-2	1.16-1.10	H-2, H-11 (2H, *m*)
21	28.2	C-28	0.98	Me-28 (3H, *s*)
22	26.9	C-7	2.37-2.31	H-7, H-7 (2H, *m*)
23	25.8	C-12		
24	22.9	C-22	2.08-2.05	2x H-22 (2H, *m*)
25	22.4	C-29	0.89	Me-29 (3H, *s*)
26	19.2	C-30	1.01	Me-30 (3H, *s*)
27	18.3	C-6		
28	17.3	C-19	0.90	Me-19 (3H, *s*)
29	15.8	C-18	0.76	Me-18 (3H, *s*)
30	15.46	C-21	0.94	Me-21 (3H, *d*, J=7.5 Hz)
31	12.93	C-27	1.87	Me-27 (3H, *d*, J=1.5 Hz)

proliferation. Methyl-3α,23-dihydroxy-17,14-friedolanstan-8,14,24-trien-26-oat was evaluated for its effect on the proliferation of MCF-7 breast cancer cell lines by the MTT assay. The evaluation resulted in a time- and dose-dependent manner inhibition of the compound on the cell proliferation (Fig. 2). The compound strongly inhibited the MCF-7 cell line proliferation in 24 and 48 h treatments, with the IC_{50} value of 82 and 70 μM in the 24 and 48 h measurements, respectively.

Proapoptotic activity of methyl-3α,23-dihydroxy-17,14-friedolanstan-8,14,24-trien-26-oat through PARP protein activation. The MTT assay showed strong inhibitory activity of methyl-3α,23-dihydroxy-17,14-friedolanstan-8,14,24-trien-26-oat against the MCF-7 cell line proliferation, thus, the compound was further examined for its proapoptotic activity through PARP protein activation within 24 and 48 h of treatment. The inhibition of MCF-7 human breast cancer cells proliferation by the compound was mediated by the induction of apoptosis, marked by PARP protein activation, which is one of the most optimal biomarkers of apoptosis. Furthermore, the compound also inhibited the expression of Akt oncogene (Fig. 3).

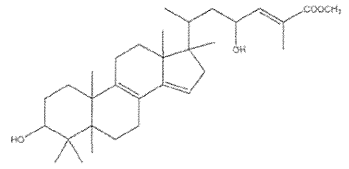

Figure 1. Methyl-3α,23-dihydroxy-17,14-friedolanstan-8,14,24-trien-26-oat isolated from *G. celebica* leaves.

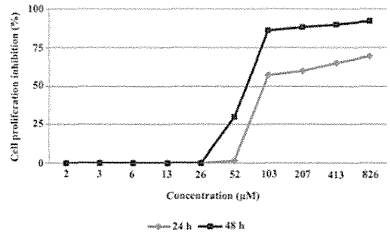

Figure 2. Effects of 24 and 48 h treatments of methyl-3α,23-dihydroxy-17,14-friedolanstan-8,14,24-trien-26-oat obtained from the *G. celebica* leaves on the proliferation of MCF-7 breast cancer cell lines.

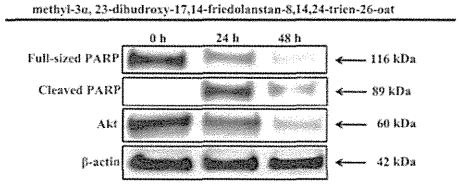

Figure 3. Pro-apoptotic activity of methyl-3α,23-dihydroxy-17,14-friedolanstan-8,14,24-trien-26-oat obtained from the *G. celebica* leaves.

Discussion

Traditional medicinal plants have long been regarded as a source of potential therapeutic agents, and the search for new drugs is usually based on this approach (13). In drug discovery, our previous studies recently applied a new approach of selecting plants based on the use of those plants by primates (3,5). In our previous study, the extracts of the *G. celebica* leaves were strongly cytotoxic to the MCF-7 breast

cancer cell line (6). Thus, these extracts had the potential for further investigation.

The present study was focused on identifying an antiproliferative compound from the *G. celebica* leaves. This study resulted in the isolation of a friedolanostane triterpenoid, methyl-3α, 23-dihydroxy-17,14-friedolanstan-8,14,24-trien-26-oat, which strongly inhibited the MCF-7 cell line proliferation in a time- and dose-dependent manner, with IC_{50} values of 82 and 70 μM in the 24 and 48 h treatments, respectively.

This compound has not been reported previously in connection with its cytotoxicity in these cancer cell lines. Through investigating the anticancer activities of *Garcinia* plants, numerous studies have focused on xanthone derivatives, which are the main compounds of any *Garcinia* species (14-16). These findings will thus be valuable supporting information for revealing the efficacy of *Garcinia* species as a potential anticancer source.

In the present study, this compound was also found to induce the apoptosis of MCF-7 cells, which was indicated by the changes in the expression levels of PARP. The expression levels of PARP were analyzed after 24 and 48 h of treatment. The N-terminal fragment of PARP, which is an 89-kDa peptide cleaved from full-length PARP (116 kDa), was detected as early as 24 h after treatment of the MCF-7 cells with methyl-3α, 23-dihydroxy-17,14-friedolanstan-8,14,24-trien-26-oat. Akt, as one of the most important survival signaling pathways in malignancy, has an important role in determining the chemosensitivity of cancer cells. These survival signaling proteins were decreased by treatment with methyl-3α,23-dihydroxy-17,14-friedolanstan-8,14,24-trien-26-oat, as shown by the reduced expression of the Akt protein.

However, the present study is not without limitations. A detailed mechanism regarding the effect of methyl-3α,23-dihydroxy-17,14-friedolanstan-8,14,24-trien-26-oat on the expression of several proteins that may directly be affected were not performed, including pro- or anti-apoptotic, estrogen receptor α and phosphorylated Akt (Ser473) proteins.

In conclusion, the present results suggest that methyl-3α,23-dihydroxy-17,14-friedolanstan-8,14,24-trien-26-oat inhibited the growth of MCF-7 cells through the induction of apoptosis and downregulation of the oncogene Akt. Further evaluation of its toxicity and detailed mechanisms of its antiproliferative action is required to provide a scientific basis for its chemopreventive and chemotherapeutic application in breast cancer management.

Acknowledgements

The present study was financially supported by the Directorate General of Higher Education of the Ministry of Education and Culture of Indonesia (Grand-in-Aid for the International Research Collaborations and Publications; grant no. 430/SP2H/PP/DP2 M/VII/2010) for AS.

References

1. Sakarkar DM and Deshmukh VN: Ethnopharmacological review of traditional medicinal plants for anticancer activity. Int J Pharm Tech Res 3: 298-308, 2011.
2. Kinghorn AD, Chai HB, Sung CK and Keller WJ: The classical drug discovery approach to defining bioactive constituents of botanicals. Fitoterapia 82: 71-79, 2011.
3. Koshimizu K, Murakami A, Hayashi H, *et al*: Biological activities of edible and medicinal plants from Indonesia and Malaysia. In: Proceedings of The Tokyo International Forum on Conservation and Sustainable Use of Tropical Bioresources, Tokyo, pp203-208, 1998.
4. Ferlay J, Shin HR, Bray F, Forman D, Mathers C and Parkin DM: Estimates of worldwide burden of cancer in 2008: GLOBOCAN 2008. Int J Cancer 127: 2893-2917, 2010.
5. Diantini A, Subarnas A, Lestari K, Halimah E, Susilawati Y, Supriyatna, Julaeha E, Achmad TH, Suradji EW, Yamazaki C, *et al*: Kaempferol-3-O-rhamnoside isolated from the leaves of *Schima wallichii* Korth. Inhibits MCF-7 breast cancer cell proliferation through activation of the caspase cascade pathway. Oncol Lett 3: 1069-1072, 2012.
6. Subarnas A, Diantini A, Abdulah R, *et al*: Antiproliferative activity of primates-consumed plants against MCF-7 human breast cancer cell lines. E3 J Med Res 1: 38-43, 2012.
7. Meyer BN, Ferrigni NR, Putnam JE, Jacobsen LB, Nichols DE and McLaughlin JL: Brine shrimp: A convenient general bioassay for active plant constituents. Planta Med 45: 31-34, 1982.
8. Abdulah R, Faried A, Kobayashi K, Yamazaki C, Suradji EW, Ito K, Suzuki K, Murakami M, Kuwano H and Koyama H: Selenium enrichment of broccoli sprout extract increases chemosensitivity and apoptosis of LNCaP prostate cancer cells. BMC Cancer 9: 414, 2009.
9. Shiao MS, Lin LJ and Yeh SF: Triterpenes in *Ganoderma lucidum*. Phytochemistry 27: 873-875, 1988.
10. Lin LJ, Shiao MS and Yeh SF: Triterpenes from *Ganoderma lucidum*. Phytochemistry 27: 2269-2271, 1988.
11. Rukachaisirikul V, Adair A, Dampawan P, Taylor WC and Turner PC: Lanostanes and friedolanostanes from the pericarp of *Garcinia hombroniana*. Phytochemistry 55: 183-188, 2000.
12. Rukachaisirikul V, Saelim S, Karnsomchoke P and Phongpaichit S: Friedolanostanes and lanostanes from the leaves of *Garcinia hombroniana*. J Nat Prod 68: 1222-1225, 2005.
13. Fabricant DS and Farnsworth NR: The value of plants used in traditional medicine for drug discovery. Environ Health Perspect 109 (Suppl 1): S69-S75, 2001.
14. Matsumoto K, Akao Y, Ohguchi K, Ito T, Tanaka T, Iinuma M and Nozawa Y: Xanthones induce cell-cycle arrest and apoptosis in human colon cancer DLD-1 cells. Bioorg Med Chem 13: 6064-6069, 2005.
15. Suksamrarn S, Komutiban O, Ratananukul P, Chimnoi N, Lartpornmatulee N and Suksamrarn A: Cytotoxic prenylated xanthones from the young fruit of *Garcinia mangostana*. Chem Pharm Bull (Tokyo) 54: 301-305, 2006.
16. Akao Y, Nakagawa Y, Iinuma M and Nozawa Y: Anti-cancer effects of xanthones from pericarps of mangosteen. Int J Mol Sci 9: 355-370, 2008.

Surg Endosc
DOI 10.1007/s00464-016-4747-7

Feasibility of laparoscopic liver resection for caudate lobe: technical strategy and comparative analysis with anteroinferior and posterosuperior segments

Kenichiro Araki[1,2] · David Fuks[1] · Takeo Nomi[1,3] · Satoshi Ogiso[1,4] · Ruben R. Lozano[1] · Hiroyuki Kuwano[2] · Brice Gayet[1]

Received: 15 October 2015 / Accepted: 4 January 2016

Abstract
Background Although laparoscopic liver resection (LLR) is now considered a standard procedure in peripheral segments, there are few reports on laparoscopic segment 1 (Sg1) resection. The aim of this study was to assess both safety and feasibility of Sg1 LLR.
Methods From 2000 to 2014, all patients who underwent LLR were identified from a prospective database. Patients with resection of Sg1 (Sg1 group) were compared with those with resection of anteroinferior segments (AI group: segments 3, 4b, 5, 6) or posterosuperior segments (PS group: segments 4a, 7, 8), in terms of tumor characteristics, surgical treatment, and short-term outcomes.
Results There were 15, 151, and 67 patients in Sg1, AI, and PS groups. Tumor size and tumor number were similar between the three groups ($p = 0.139$, $p = 0.102$). Operative time was significantly shorter in Sg1 (150 min) and AI group (135 min) compared with PS group (180 min) ($p = 0.021$). Median blood loss was notably higher in PS group (140 ml) compared with Sg1 group (75 ml) and AI group (10 ml) ($p = 0.001$). No mortality was observed in all groups. Postoperative complication rate was 20.0 % with Sg1 group, 14.6 % with AI group, and 20.9 % with PS group ($p = 0.060$). The rate of major complication was significantly higher in Sg1 group (13.3 %) and PS group (11.9 %) compared with AI group (4.0 %) ($p = 0.042$). Resection margins were clear in all Sg1 and PS group patients, whereas two (1.3 %) patients in AI group had R1 margins ($p = 0.586$).
Conclusion The laparoscopic approach of isolated resection located in the caudate lobe is a feasible and curative surgical option in selected patients.

Keywords Laparoscopic liver resection · Caudate lobe · Anteroinferior lesion · Posterosuperior lesion · Caudal approach

The caudate lobe (Couinaud's segment 1: Sg1) is a small liver segment consisting of three parts: Spiegel's lobe, paracaval portion, and caudate process. Sg1 is anatomically unique in that it is situated posteriorly in the liver and directly over the inferior vena cava (IVC), which makes this lobe not directly visible and less accessible for surgeons. In addition, Sg1 contains several thin hepatic veins draining directly into IVC, which increases the risk of bleeding in dissecting the attachment between Sg1 and IVC [1]. Due to these anatomical characteristics, local excision of Sg1 is technically demanding and requires different surgical strategies for each individual case [2].

Despite diffusion of laparoscopic liver resection (LLR), there have been a few reports on laparoscopic Sg1 resection [3, 4]. The aim of this study was to assess the safety and feasibility of the procedure by comparing its outcomes

✉ Brice Gayet
brice.gayet@imm.fr

Kenichiro Araki
karaki@gunma-u.ac.jp

[1] Department of Digestive Diseases, Institut Mutualiste Montsouris, Paris Descartes University, 42 Boulevard Jourdan, 75014 Paris, France

[2] Department of General Surgical Science, Gunma University Graduate School of Medicine, Maebashi, Gunma, Japan

[3] Department of Surgery, Nara Medical University, Nara, Japan

[4] Division of Hepato-Biliary-Pancreatic Surgery and Transplantation, Department of Surgery, Graduate School of Medicine, Kyoto University, Kyoto, Japan

Published online: 28 January 2016

to those after laparoscopic resection of anteroinferior and posterosuperior segment.

Materials and methods

Study population

From January 2000 to December 2014, all patients who underwent LLR at author's institution were identified from a prospective database, and their data were retrospectively reviewed. Patients with resection of segment 1 (Sg1 group) were compared with those with resection of anteroinferior segments (AI group: segment 3, 4b, 5, 6) or posterosuperior segments (PS group: segment 4a, 7, 8), in terms of tumor characteristics, surgical treatment, and short-term outcomes. Suitability for the laparoscopic approach was based on tumor size and location, type of planned resection, and patient comorbidities. Except unusual cases with limited tumor abutment on IVC, direct involvement of IVC on preoperative imaging was considered as a contraindication to laparoscopic approach.

Preoperative evaluation

Preoperative investigations included blood and liver function tests, as well as routine cardiorespiratory evaluations. Computed tomography imaging of the thorax, abdomen, and pelvis was obtained routinely. In recent years, magnetic resonance imaging of the liver was routinely performed. No specific evaluation was required for Sg1 resection, but special attention was payed on contact between the tumor and IVC.

Surgical procedures

The surgical technique of LLR, including the positioning of the trocars, has been previously described [5, 6]. Intra-abdominal pressure was maintained at 12 mmHg. Liver resectability was routinely confirmed by intra-operative ultrasonography [7]. The gastrohepatic ligament is divided to approach segment I, preserving the accessory left hepatic artery. The hepatoduodenal ligament is dissected posteriorly, and the portal pedicles going toward segment I are identified, dissected free, and divided. The caudate lobe is mobilized from the left side and also along the anterior aspect of the IVC, dividing the short hepatic veins. The hepatic veins are usually coagulated without any clip and/or suture. The confluence of the left and middle hepatic vein with the IVC is exposed after division of the segment I hepatic vein; the duct of Arantius is cut or preserved depending on the tumor location. Then, the liver parenchyma is dissected from the caudal side toward the IVC, exposing the posterior aspect of the middle hepatic vein [8]. For all procedures, tissue dissection and hemostasis were performed using an ultrasonic dissector, such as the Harmonic scalpel (Ethicon Endo-Surgery, Inc., Cincinnati, OH) or, more recently, the Thunderbeat® (Olympus Co, Tokyo); Gayet bipolar forceps (MicroFrance CEV134, Medtronic, Minneapolis, MN) provided retraction and rescue hemostasis. All intra-operative parameters, including type and duration of vascular clamping, blood loss with subsequent intraoperative blood transfusion, and duration of surgery, were recorded. The overall surgical policy was to attempt radical anatomic or wedge resection, sparing the greatest amount of liver parenchyma feasible.

Postoperative outcomes

Postoperative complications after LLR were stratified according to the Dindo–Clavien classification, and major complications were defined as a grade $\geq$ III [9]. If a patient had two or more complications, the most severe was taken in account. Liver-specific complications were detailed as follows: Liver failure was defined according to the "50–50 criteria" on postoperative day 5 [10], ascites was defined as abdominal drainage output of >10 ml per kg per day after postoperative day 3, and biliary leakage was defined as a bilirubin concentration in the drainage fluid of more than threefold that in serum [11]. Complications and operative mortality were considered if they occurred within 90 days of surgery or at any time during the postoperative hospital stay.

Statistical analysis

Patient baseline characteristics were expressed as mean (SD) for continuous data and numbers with percentages for categorical data. Preoperative, operative, and postoperative characteristics were compared. Chi-square test was used to identify differences in categorical variables, and ANOVA was used to compare differences in categorical variables. Cumulative overall survival rates were determined using the Kaplan–Meier method and compared using the log-rank test. All statistical analyses were performed using SPSS for Windows version 21.0 (SPSS Inc.), and statistical significance was accepted at the 0.05 level.

Results

Preoperative characteristics

Of 233 patients included in this study cohort, there were 15, 151, and 67 patients in the Sg1, AI, and PS groups, respectively. Preoperative characteristics of these patients

are detailed in Table 1. The three groups did not differ significantly in terms of demographics and tumor characteristics. The rate of previous abdominal surgery was significantly higher in PS group (73.1 %) compared with Sg1 (46.6 %) and AI groups (48.3 %) ($p = 0.002$). Tumor characteristics including indication and tumor number were similar in each group, and tumor diameter was also similar in each group: Sg1 group (19.5 mm), AI group (20.0 mm), and PS group (25.0 mm), respectively ($p = 0.139$). There was no difference in the proportion of patients having previous hepatectomy (13.3 vs. 14.6 vs. 23.9 %, $p = 0.220$).

Intra-operative characteristics

The number of patients who underwent anatomical liver resection was 3 (20.0 %) in the Sg1 group, 26 (17.2 %) in the AI group, and 20 (29.9 %) in the PS group ($p = 0.590$). There was no difference in the extra-hepatic procedures performed. No patient required vascular reconstruction. Operative time was shorter in the Sg1 (150 min) and AI group (135 min) compared with PS group (180 min) ($p = 0.021$). Median blood loss was larger in the PS group (140 ml, range 0–1500 ml) compared with Sg1 group (75 ml, range 0–500 ml) and AI group (10 ml, range 0–1100 ml) ($p = 0.001$) (Table 2). There was no significant difference in use of intra-operative transfusion. Two patients required conversion in the PS group (3.0 %) and none in Sg1 and AI groups. Resection margins were clear in all Sg1 and PS group patients, whereas two (1.3 %) patients had R1 margins in AI group ($p = 0.586$).

Postoperative outcomes

There was no mortality in the three groups. Three (20.0 %) patients in Sg1 group experienced postoperative

Table 1 Preoperative characteristics

	N (%)			*p* value
	Sg1 group ($N = 15$)	AI group ($N = 151$)	PS group ($N = 67$)	
Age, year, mean ± SD	64 ± 9	59 ± 15	62 ± 13	0.624
Male gender	7 (46.6)	84 (55.6)	38 (56.7)	0.944
BMI, kg/m^2, mean ± SD	25.3 ± 4.7	25.4 ± 4.4	26.2 ± 5.0	0.700
Alcohol	3 (20.0)	33 (21.9)	12 (17.9)	0.624
Smoking	3 (20.0)	22 (14.6)	11 (16.4)	0.664
Comorbidities				
Diabetes mellitus	1 (6.6)	8 (5.3)	9 (13.4)	0.109
Hypertension	3 (20.0)	27 (17.9)	17 (25.4)	0.374
Dyslipidemia	2 (13.3)	23 (15.2)	10 (14.9)	0.760
Ischemic heart disease	0 (0)	10 (6.6)	4 (6.0)	0.632
COPD	1 (6.6)	4 (2.6)	2 (3.0)	0.601
Preoperative chemotherapy	3 (20.0)	41 (27.2)	11 (16.4)	0.236
Viral status				
HBV	0	1 (0.7)	1 (1.5)	0.776
HCV	0	2 (1.3)	1 (1.5)	0.907
Diagnosis				
CRLM	10 (66.6)	93 (61.6)	43 (64.2)	0.168
Other metastases	2 (13.3)	25 (16.6)	9 (13.4)	0.514
HCC	1 (6.6)	9 (6.0)	7 (10.4)	0.465
Cholangiocarcinoma	0 (0)	4 (2.6)	0 (0)	0.349
Benign disease	2 (13.3)	20 (13.2)	8 (11.9)	0.187
Previous abdominal surgery	7 (46.6)	73 (48.3)	49 (73.1)	0.002
Previous hepatectomy	2 (13.3)	22 (14.6)	16 (23.9)	0.220
Tumor size, mm, median (range)	19.5 (2–50)	20.0 (5–160)	25.0 (8–140)	0.139
Tumor number, median (range)	1.0 (1–2)	1.0 (1–4)	1.0 (1–4)	0.102

BMI body mass index, *COPD*, chronic obstructive pulmonary disease, *HBV* hepatitis B virus, *HCV* hepatitis C virus, *CRLM*, colorectal cancer liver metastases, *HCC* hepatocellular carcinoma

Table 2 Intra-operative characteristics

	N (%)			*p* value
	Sg1 group (*N* = 15)	AI group (*N* = 151)	PS group (*N* = 67)	
Surgical procedures				
Pure laparoscopy	13 (86.7)	123 (81.5)	59 (88.1)	0.492
Anatomical resection	3 (20.0)	26 (17.2)	20 (29.9)	0.590
Use of Pringle maneuver	0	2 (1.3)	0	0.590
Blood loss, ml, median (range)	75 (0–500)	10 (0–1100)	140 (0–1500)	0.001
Operative time, min, median (range)	150 (60–480)	135 (60–480)	180 (60–600)	0.021
Intraoperative transfusion	0	0	3 (4.5)	0.022
Conversion	0	0	2 (3.0)	0.082
Abdominal drainage	0	5 (3.3)	2 (3.0)	0.801

complications, 22 (14.6 %) of the AI group, and 14 (20.9 %) of the PS group ($p = 0.060$) (Table 3). The rate of major complication was significantly higher in the Sg1 group (13.3 %, $N = 2$) and PS group (11.9 %, $N = 8$) compared with AI group (4.0 %, $N = 6$) ($p = 0.042$). One Sg1 patient who underwent combined lymphadenectomy developed pancreatic fistula, and this patient needed reoperation for management of this complication. Three patients in AI group and one patient in PS group required reoperation for a complication in relation to simultaneous colorectal resection. Bile leakage was observed in one patient in the AI group (0.7 %) and two PS group patients (3.0 %) ($p = 0.218$), managed by abdominal drainage. Biliary stenosis was occurred in one patient in the Sg1 group (6.6 %), successfully treated by endoscopic stenting. The length of hospital stay was significantly longer in Sg1 group (8.0 ± 6.5 days) and PS group (8.3 ± 7.3 days) compared with AI group (6.7 ± 5.1 days) ($p = 0.008$).

As shown in Table 4, Sg1 resection was not identified as an independent factor associated with postoperative major morbidity unlike PS resection. Based on multivariate analysis, COPD was found to be an independent predictor for major complication.

Discussion

As a result of this unique anatomical location, caudate lobe resection is technically challenging, because it is easy to damage the bile ducts and an error in dissecting the posterior part of the caudate lobe can cause uncontrolled bleeding from the IVC [12]. However, precise anatomical knowledge of the caudate segment, improvements in perioperative care, and refined surgical technique for caudate lobectomy in open surgery have resulted in more widespread use of this procedure. Until recently, the most favorable locations for LLR have been the peripheral liver segments [13]. However, the limitations associated with the procedure have gradually diminished with the accumulation of surgical experience in LLR. Although the reports are limited, LLR has been shown to be a feasible option for lesions located in the posterior and superior segments [14–16]. In laparoscopic view, the surgical field is visualized and accessed from the caudal side to the cranial side using a laparoscope, known as the 'caudal approach.' Thus, laparoscopic approach for caudate lobe has advantage of easy access to this location compared with approach for cranial side, such as posterosuperior segments [17–19]. However, the Sg1 is close to the liver hilum, major hepatic veins, and IVC, and is still considered theoretically as a contraindication for laparoscopic approach. Indeed, parenchymal transection near these major vessels poses greater risk of injury, and once such an injury occurs, the complications may be difficult to control laparoscopically.

The present study represents the first series reporting the results of laparoscopic Sg1 resection and the analysis compared with other lesions. Indeed, this study suggests that LLR can be safely performed for Sg1 tumors without open conversion or mortality. When compared with AI and PS groups, the Sg1 group showed a similar operative time, a significant reduction in blood loss, and a similar rate of intraoperative transfusion.

Although the danger in resection of the caudate lobe may arise from massive bleeding from the anterior part of the IVC and posterior part of the middle hepatic vein, laparoscopy has the significant advantages of providing excellent view and access to these parts behind the liver by 'caudal approach' [17–19]. Indeed, the laparoscopic approach allows precise dissection upward along the IVC. At this level, short hepatic veins for Sg1 are meticulously coagulated with the bipolar forceps and then divided rather

Table 3 Comparisons between postoperative outcomes

	N (%)			*p* value
	Sg1 group (*N* = 15)	AI group (*N* = 151)	PS group (*N* = 67)	
Postoperative mortality	0	0	0	–
Overall complication[a]	3 (20.0)	22 (14.6)	14 (20.9)	0.060
Infectious complications	2 (13.3)	7 (4.6)	8 (11.9)	0.021
Major complication[a]	2 (13.3)	6 (4.0)	8 (11.9)	0.042
Overall complication				
Liver-specific complication				
Biliary leakage	0	1 (0.7)	2 (3.0)	0.336
Intra-abdominal abscess	0	4 (2.6)	5 (7.5)	0.172
Biliary stenosis	1 (6.6)	0	0	0.001
Postoperative bleeding	0	0	1 (1.5)	0.293
Pancreatic fistula	1 (6.6)	0	0	0.001
Pulmonary complication	0	1 (0.7)	1 (1.5)	0.487
Pleural effusion	0	1 (0.7)	2 (3.0)	0.344
Ileus	1 (6.6)	4 (2.6)	0	0.172
Anastomotic leakage	0	1 (0.7)	0	0.766
General complication	0	10 (6.6)	3 (4.5)	0.542
Postoperative major complication[a]				
Liver-specific complication				
Biliary leakage	0	1 (0.7)	2 (3.0)	0.336
Intra-abdominal abscess	0	2 (1.3)	3 (4.5)	0.172
Biliary stenosis	1 (6.6)	0	0	0.001
Postoperative bleeding	0	0	1 (1.5)	0.293
Pancreatic fistula	1 (6.6)	0	0	0.001
Pulmonary complication	0	0	1 (1.5)	0.293
Pleural effusion	0	0	1 (1.5)	0.293
Anastomotic leakage	0	1 (0.7)	0	0.766
Stenosis of stomach	0	1 (0.7)	0	0.766
Ileus	0	1 (0.7)	0	0.766
Reoperation	1 (6.6)	3 (2.0)	1 (1.5)	0.364
Length of hospital stay, days, mean ± SD	8.0 ± 6.5	6.7 ± 5.1	8.3 ± 7.3	0.008

[a] Postoperative complications were stratified according to the Clavien–Dindo classification, which defines major complications by grade III or more

than clipped. We believe that clips, even locked clips, could easily slip when applied on very short veins. The posterior part of the middle hepatic vein is more inaccessible. Improved laparoscopic vision (particularly via three-dimensional camera) and the flexibility of the camera further facilitate meticulous dissection of the liver parenchyma even in the narrow surgical field at the front of the IVC and behind the liver [20].

Additionally, postoperative complications were comparable in the three groups. However, we observed nonsignificant higher rates of infectious complications and reoperation after Sg1 resection. This absence of significance may be explained by the limited sample size. However, even though Sg1 resection is scarce uncommon, we observed complications could be assigned specifically to Sg1 resection; this was the case of a postoperative biliary stricture developed by a patient six weeks after caudate lobectomy and successfully treated by biliary stenting. Indeed, we have to keep in mind that biliary drainage for Sg1 includes small tributaries to the right but occurs predominantly through the left hepatic duct [21]. Postoperative morbidity after Sg1 resection is similar to those observed after PS resection and higher than those observed after AI resection. Therefore, we should consider Sg1 as arduous location for laparoscopic approach.

Table 4 Logistic regression analysis for the risk of major complication

Risk factors	Variables	Univariate analysis			Multivariate analysis		
		p value	Odds ratio	95 % CI	*p* value	Odds ratio	95 % CI
Age (years)	≤65 versus >65	0.134	2.824	0.727–10.973			
Gender	Male versus Female	0.597	0.708	0.256–1.962			
BMI (kg/m^2)	≤30 versus >30	0.803	1.333	0.139–12.758			
Preoperative complication							
Diabetes mellitus	Negative versus positive	0.808	0.773	0.096–6.209			
Hypertension	Negative versus positive	0.897	0.918	0.250–3.364			
Dyslipidemia	Negative versus positive	0.338	0.366	0.047–2.863			
Ischemic heart disease	Negative versus positive	0.999	0.000	–			
COPD	Negative versus positive	0.043	5.943	1.057–33.415	0.033	7.319	1.178–45.480
Preoperative chemotherapy	Negative versus positive	0.128	2.209	0.795–6.136			
Previous abdominal surgery	Negative versus positive	0.129	2.462	0.769–7.878			
Previous hepatectomy	Negative versus positive	0.249	0.299	0.038–2.333			
Tumor size (mm)	≤30 versus >30	0.428	0.987	0.956–1.019			
Anatomical resection	negative versus positive	0.331	1.734	0.572–5.256			
Operation time (min)	≤300 versus >300	0.414	1.003	0.996–1.009			
Blood loss (ml)	≤500 versus >500	0.055	1.001	1.000–1.003	0.221	1.001	0.999–1.003
Sg1 group	Negative versus positive	0.233	0.377	0.076–1.871			
PS group	Negative versus positive	0.063	0.378	0.136–1.054	0.076	0.334	0.100–1.122

BMI body mass index, *COPD* chronic obstructive pulmonary disease

Another concern about the application of LLR for tumors located in Sg1 is the ability to obtain a safe resection margin. Indeed, LLR for tumors close to both the hilum and the major hepatic veins are technically challenging procedures because it may be difficult to obtain adequate surgical margins, even in open liver resection [13]. The present study emphasizes that en bloc complete caudate lobectomy involving the caudate lobe is not appropriate in all cases since all 15 patients who underwent Sg1 resection had clear surgical margins. In addition, laparoscopic ultrasound should be widely used during the procedure in order to provide a precise evaluation of tumor location and its relationship with the adjacent vascular structures [7].

The limitations of the present series include both the limited number of patients who underwent Sg1 resection and the relative heterogeneity of the tumors. Additionally, patients were highly selected given only one had cirrhosis and all tumor diameters were under 3 cm. Even though it would have been ideal to compare intra- and postoperative outcomes between laparoscopic and open Sg1 resection, our institute has high volume number of LLR; the total number of Sg1 liver resection is very low. We assume that it is a limitation of this study. Furthermore, we emphasize that surgeons should have experienced technique of LLR when considering laparoscopic Sg1 resection.

In conclusion, this study suggests that the laparoscopic approach is a feasible and curative surgical option for resection of tumors located in the caudate lobe with acceptable operative time, postoperative outcomes, and tumor-free margins in selected patients.

Acknowledgments We thank Dr. Mahendran Govindasamy for coordinating patient's follow-up and maintaining the prospective database that formed the basis of this study.

Compliance with ethical standards

Disclosures Kenichiro Araki, David Fuks, Takeo Nomi, Satoshi Ogiso, Ruben R Lozano, Hiroyuki Kuwano, and Brice Gayet have no conflict of interest. Brice Gayet is consultant for Olympus.

References

1. Kumon M (1985) Anatomy of the caudate lobe with special reference to portal vein and bile duct. Acta Hepatol Jap 26:1193–1199
2. Kosuge T, Yamamoto J, Takayama T, Shimada K, Yamasaki S, Makuuchi M, Hasegawa H (1994) An isolated, complete resection of the caudate lobe, including the paracaval portion, for hepatocellular carcinoma. Arch Surg 129:280–284
3. Dulucq JL, Wintringer P, Stabilini C, Mahajna A (2006) Isolated laparoscopic resection of the hepatic caudate lobe: surgical technique and a report of 2 cases. Surg Laparosc Endosc Percut Tech 16:32–35

4. Kokkalera U, Ghellai A, Vandermeer TJ (2007) Laparoscopic hepatic caudate lobectomy. J Laparoendosc Adv Surg Tech A 17:36–38
5. Nomi T, Fuks D, Govindasamy M, Mal F, Nakajima Y, Gayet B (2015) Risk factors for complications after laparoscopic major hepatectomy. Br J Surg 102:254–260
6. Nomi T, Fuks D, Kawaguchi Y, Mal F, Nakajima Y, Gayet B (2015) Learning curve for laparoscopic major hepatectomy. Br J Surg 102:796–804
7. Araki K, Conrad C, Ogiso S, Kuwano H, Gayet B (2014) Intraoperative ultrasonography of laparoscopic hepatectomy: key technique for safe liver transection. J Am Coll Surg 218:e37–e41
8. Ishizawa T, Gumbs AA, Kokudo N, Gayet B (2012) Laparoscopic segmentectomy of the liver: from segment I to VIII. Ann Surg 256:959–964
9. Dindo D, Demartines N, Clavien PA (2004) Classification of surgical complications: a new proposal with evaluation in a cohort of 6336 patients and results of a survey. Ann Surg 240:205–213
10. Balzan S, Belghiti J, Farges O, Ogata S, Sauvanet A, Delefosse D, Durand F (2005) The "50–50 criteria" on postoperative day 5: an accurate predictor of liver failure and death after hepatectomy. Ann Surg 242:824–828, discussion 828–829
11. Koch M, Garden OJ, Padbury R, Rahbari NN, Adam R, Capussotti L, Fan ST, Yokoyama Y, Crawford M, Makuuchi M, Christophi C, Banting S, Brooke-Smith M, Usatoff V, Nagino M, Maddern G, Hugh TJ, Vauthey JN, Greig P, Rees M, Nimura Y, Figueras J, DeMatteo RP, Buchler MW, Weitz J (2011) Bile leakage after hepatobiliary and pancreatic surgery: a definition and grading of severity by the International Study Group of Liver Surgery. Surgery 149:680–688
12. Yanaga K, Matsumata T, Hayashi H, Shimada M, Urata K, Sugimachi K (1994) Isolated hepatic caudate lobectomy. Surgery 115:757–761
13. Yoon YS, Han HS, Cho JY, Kim JH, Kwon Y (2013) Laparoscopic liver resection for centrally located tumors close to the hilum, major hepatic veins, or inferior vena cava. Surgery 153:502–509
14. Huang MT, Lee WJ, Wang W, Wei PL, Chen RJ (2003) Hand-assisted laparoscopic hepatectomy for solid tumor in the posterior portion of the right lobe: initial experience. Ann Surg 238:674–679
15. Yoon YS, Han HS, Cho JY, Ahn KS (2010) Total laparoscopic liver resection for hepatocellular carcinoma located in all segments of the liver. Surg Endosc 24:1630–1637
16. Ogiso S, Conrad C, Araki K, Nomi T, Anil Z, Gayet B (2015) Laparoscopic transabdominal with transdiaphragmatic access improves resection of difficult posterosuperior liver lesions. Ann Surg 262:358–365
17. Wakabayashi G, Cherqui D, Geller DA, Han HS, Kaneko H, Buell JF (2014) Laparoscopic hepatectomy is theoretically better than open hepatectomy: preparing for the 2nd international consensus conference on laparoscopic liver resection. J Hepatobiliary Pancreat Sci 21:723–731
18. Soubrane O, Schwarz L, Cauchy F, Perotto LO, Brustia R, Bernard D, Scatton O (2015) A conceptual technique for laparoscopic right hepatectomy based on facts and oncologic principles: the caudal approach. Ann Surg 261:1226–1231
19. Ogiso S, Nomi T, Araki K, Conrad C, Hatano E, Uemoto S, Fuks D, Gayet B (2015) Laparoscopy-specific surgical concepts for hepatectomy based on the laparoscopic caudal view: a key to reboot surgeons' minds. Ann Surg Oncol 22:327–333
20. Velayutham V, Fuks D, Nomi T, Kawaguchi Y, Gayet B (2016) 3D visualization reduces operating time when compared to high-definition 2D in laparoscopic liver resection: a case-matched study. Surg Endosc 30:147–153
21. Chaib E, Ribeiro MA Jr, Silva Fde S, Saad WA, Cecconello I (2007) Surgical approach for hepatic caudate lobectomy: review of 401 cases. J Am Coll Surg 204:118–127

Cancer Science
Japanese Cancer Association JCA
Open Access

Establishment of a novel method to evaluate peritoneal microdissemination and therapeutic effect using luciferase assay

Ryo Takahashi,[1] Takehiko Yokobori,[1,2] Katsuya Osone,[1] Hironori Tatsuki,[1] Takahiro Takada,[1] Toshinaga Suto,[1] Reina Yajima,[1] Toshihide Kato,[1] Takaaki Fujii,[1] Souichi Tsutsumi,[1] Hiroyuki Kuwano[1] and Takayuki Asao[3]

Departments of [1]General Surgical Science; [2] Molecular Pharmacology and Oncology; [3] Oncology Clinical Development, Graduate School of Medicine, Gunma University, Maebashi, Japan

Key words

Colon 26, luciferase assay, microdissemination, mouse model, peritoneal dissemination

Correspondence

Takehiko Yokobori, Department of General Surgical Science, Gunma University, Graduate School of Medicine, 3-39-22 Showa-machi, Maebashi, Gunma 371-8511, Japan.
Tel: +81-27-220-8224; Fax: +81-27-220-8230;
E-mail: bori45@gunma-u.ac.jp

Funding Information

Uehara Memorial Foundation; Ministry of Education, Culture, Sports, Science and Technology (Promotion Plan for the Platform of Human Resource Development for Cancer); Japan Society for the Promotion of Science (15K10085 and 22591450).

Received December 2, 2015; Revised December 22, 2015; Accepted December 24, 2015

Cancer Sci **107** (2016) 341–346

doi: 10.1111/cas.12872

Peritoneal dissemination is a major cause of recurrence in patients with malignant tumors in the peritoneal cavity. Effective anticancer agents and treatment protocols are necessary to improve outcomes in these patients. However, previous studies using mouse models of peritoneal dissemination have not detected any drug effect against peritoneal micrometastasis. Here we used the luciferase assay to evaluate peritoneal micrometastasis in living animals and established an accurate mouse model of early peritoneal microdissemination to evaluate tumorigenesis and drug efficacy. There was a positive correlation between luminescence intensity in *in vivo* luciferase assay and the extent of tumor dissemination evaluated by *ex vivo* luciferase assay and mesenteric weight. This model has advantages over previous models because optimal luciferin concentration without cell damage was validated and peritoneal microdissemination could be quantitatively evaluated. Therefore, it is a useful model to validate peritoneal micrometastasis formation and to evaluate drug efficacy without killing mice.

Peritoneal dissemination is a major cause of recurrence in patients with colorectal, gastric, pancreatic, and ovarian cancers and is associated with a poor prognosis.[1] To improve outcomes in patients with peritoneal dissemination, clinical studies are focusing on systemic i.v. chemotherapy and/or local i.p. chemotherapy.[2–10] However, ongoing investigation of novel drugs and treatment protocols is warranted.

A number of peritoneal dissemination models have been developed to evaluate drug efficacy and toxicity in living animals with peritoneal metastasis.[11–13] However, in these models, disseminated tumor cells cannot be observed macroscopically. Therefore, it is necessary to kill the model animals to evaluate tumor spread using mesenteric weight. To reduce the need of killing experimental animals, a novel model of peritoneal dissemination to evaluate tumor spread quickly and accurately in living animals is needed.

We used the luciferase assay to evaluate the peritoneal tumors in living animals. Luciferase-expressing cancer cells are luminous, and the luciferase assay is useful to detect living cancer cells in the peritoneal cavity with high sensitivity and reproducibility. Previous studies have reported the effectiveness of luciferase assay in macroscopically observable peritoneal tumors.[14–18] However, the assay has not been used to investigate undetectable peritoneal micrometastasis. We previously reported that the adhesion of cancer cells to the peritoneum occurs within 24 h[19,20] as the first stage of peritoneal dissemination. Therefore, if invisible peritoneal microdissemination at 24 h after tumor inoculation could be detected using luciferase assay, drug efficacy against peritoneal dissemination could be quickly and accurately assessed in *in vivo* mouse models.

In this study, we developed a novel method using luciferase assay to evaluate peritoneal microdissemination and drug efficacy in a mouse model. We validated the optimal luciferin concentration that did not cause cell damage and identified a positive correlation between luminescence in *in vivo* luciferase assay and the extent of tumor dissemination. With this method, it is possible to evaluate tumorigenesis quickly and accurately and at a low cost, with reduced need to kill experimental animals.

Materials and Methods

Cell line. Colon 26-luc cells, mouse rectal carcinoma cell lines transfected with pMSCV-luc, were kindly gifted by Dr. Murakami (Division of Bioimaging Sciences, Center for

Molecular Medicine, Jichi Medical University, Tochigi, Japan) in 2010. The cells were cultured in RPMI-1640 medium (Sigma-Aldrich, Tokyo, Japan) containing 10% FBS, 50 U/mL penicillin, 50 μg/mL streptomycin (Pen strep; Gibco, Thermo Fisher Scientific, Tokyo, Japan), and 10 μg/mL puromycin (Sigma-Aldrich) at 37°C in a humid atmosphere with 5% CO_2.

Concentration of luciferin. *In vitro* and *in vivo* luciferase assays were carried out to determine the optimal administration concentration of luciferin (Ieda Trading, Tokyo, Japan). For the *in vitro* luciferase assay, 1.0×10^5 colon 26-luc cells in 50 μL medium were seeded into each well of a 96-well plate and incubated at 37°C for 24 h. Next, 50 μL/well luciferin was added at concentrations ranging from 0.008 mg/mL to 8.0 mg/mL, and images were captured after 10 min. For the *in vivo* luciferase assay, BALB/c mice were i.p. inoculated with 1.0×10^6 colon 26-luc cells in 0.5 mL PBS. On day 7, luciferin at 0.5, 1.0, or 1.5 mg/0.5 mL was injected and luminescence was observed.

Luciferin toxicity assay. To assess the toxicity of luciferin by WST-8 assay, 1.0×10^4 colon 26-luc cells in 100 μL medium were seeded into each well of a 96-well plate and incubated at 37°C for 24 h. Next, 50 μL/well luciferin at 0.25, 0.5, 1.0, 2.0, or 4.0 mg/mL was added. Sixty minutes later, luciferin was removed and culture medium (RPMI-1640) was added, and the plate was incubated at 37°C for 24 h. Cell viability was determined using a cell counting kit-8 (Dojindo, Kumamoto, Japan). Cell viability was determined by measuring the absorbance of the cells at 450 nm with the reference wavelength at 650 nm, using a Multiskan FC microplate reader (Thermo Fisher Scientific, Tokyo, Japan).

Animals. Inbred female BALB/cCrSlc mice (Japan SLC, Shizuoka, Japan) were obtained at 5 weeks of age and maintained under specific pathogen-free conditions. They were used for experiments at 6–7 weeks of age. All experiments and procedures for care and treatment of animals in this study were carried out in accordance with the requirements of the Gunma University Animal Care and Experimentation Committee (Experimental Protocol No.14-026) (Gunma University, Maebashi, Japan).

Intraperitoneal microdissemination model. As described in our previous studies, peritoneal dissemination was investigated in mice models.[11,19] Twenty BALB/c mice (nos. 1–20) were i.p. inoculated with 1.0×10^6 colon 26-luc cells in 0.5 mL PBS (day 0). On tumor implantation, cells were injected in the left lower abdomen of mice, and needles were replaced in each mouse. Twenty-four hours after injection (day 1), microdissemination was observed by *in vivo* luciferase assay. Mice with luminescence observed through the intact abdominal wall, as described below, were randomly divided into three groups: no treatment group, cisplatin (CDDP, 10 mg/kg; Sigma-Aldrich) treated group, and gemcitabine (240 mg/kg; Eli Lilly, Hyogo, Japan) treated group. Both CDDP and gemcitabine in PBS were i.p. injected into the mice on day 1. Body weights were measured on days 1, 3, 7, and 10.

***In vivo* luciferase assay and setting.** *In vivo* peritoneal microdissemination was examined using the OptimaShot CL-420α chemiluminescence imaging system (Wako, Osaka, Japan). On day 1, model mice were anesthetized with 2–5% isoflurane (Abbott Japan, Tokyo, Japan) in a custom-made box (Alfabio, Gunma, Japan; Fig. S1), and 0.5 mg luciferin (0.5 mg/mL) was injected i.p. Up to 12 mice could be placed in the box at the same time but the mice were separated by partitions to prevent interference from luminescence of neighboring mice. Luciferase assay was started within 5 min of injection of luciferin and luminescence from microdissemination was captured for 20 min. The assay was repeated on day 10, and luminescence was captured for 10 min. Luminescence intensity was calculated using Image J software (Rasband, W.S., U. S. National Institutes of Health, Bethesda, MD, USA).

***Ex vivo* luciferase assay and setting.** On day 10, *ex vivo* luciferase assay and mesenteric weight measurement were carried out to evaluate the accuracy of the *in vivo* luciferase assay. Following the *in vivo* luciferase assay, mice were killed by injuring the abdominal aorta under sufficient anesthesia. Upper, lower, and left side abdominal walls were dissected and the gastrointestinal tract from the esophagus to the rectum, and liver were resected. *Ex vivo* luciferase assay was immediately started following dissection, and luminescence was observed in four areas, the gastrointestinal tract and mesenterium, abdominal wall, retroperitoneum, and liver (Fig. S2). Luciferin 1.0 mg (1.0 mg/mL) was equally applied to the four areas and then luminescence was captured for 10 min. The number of luminescent spots was counted. Finally, the mesenteric weights were measured.

Statistical analysis. When the results of ANOVA were significant, Dunnett's multiple comparison tests were used to assess differences in luminescence intensity, numbers of luminescent spots, and body weight among the three groups. The statistical correlation between luminescence intensity, numbers of luminescent spots, and mesenteric weight was tested using Spearman's correlation coefficient. All differences were considered statistically significant if $P < 0.05$. Statistical analyses were carried out using the JMP 5 for Windows software package (SAS Institute, Tokyo, Japan).

Results

Optimal luciferin concentration was determined by *in vitro* and *in vivo* luciferase assay. *In vitro* luciferase assay showed that optimal luminescence was observed at 0.5 mg/mL (Fig. 1a). In *in vivo* luciferase assay, luminescence intensity was similar at each injection dose of luciferin (0.5, 1.0, and 1.5 mg; Fig. 1b). Cell viability was inhibited at luciferin concentrations ≥1.0 mg/mL (Fig. 1c).

Evaluation of tumor transplantation by *in vivo* luciferase assay. In *in vivo* luciferase assay, on day 1, luminescence was observed through the intact abdominal wall in 13/20 mice (65%; Fig. 2). Mice with luminescence were randomly divided into three groups. The no treatment group included mouse no. 7, 9, 10, and 17; the CDDP (10 mg/kg) group included mouse no. 4, 6, 16, and 18; and the gemcitabine (240 mg/kg) group included mouse no. 3, 8, 12, 13, and 14. On day 10, all mice with luminescence on day 1 had peritoneal dissemination validated by pathological findings, *in vivo* luciferase assay, and *ex vivo* luciferase assay. Mouse no. 10 mouse died of peritoneal dissemination on day 9.

On day 10, seven mice with no luminescence on day 1 were reexamined. Luminescence was observed in 5/7 (71.4%) of those mice (no. 1, 5, 11, 19, and 20; Fig. S3). Mouse no. 5 died on day 10; no. 11 died on day 21; and no.1, 19, and 20 died on day 24. Mouse no. 2 and 15 did not have luminescence on day 10, but mouse no. 15 died on day 28. A tumor nodule was observed in her left lower abdominal wall. On day 30, *in vivo* luciferase assay was repeated in mouse no. 2. No luminescence was observed, and no tumor nodules were observed on dissection. Therefore, the final tumor implantation rate of colon 26-luc cells was 95% (19/20).

Evaluation of drug efficacy by *in vivo* luciferase assay. In *in vivo* luciferase assay, on day 10, luminescence was observed in all three of the surviving mice in the no treatment group, in

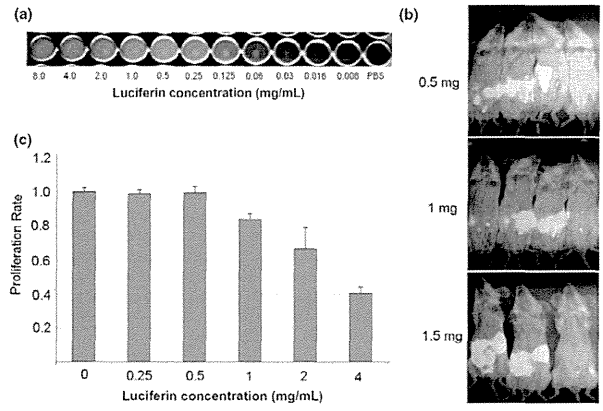

Fig. 1. Determination of the optimal concentration of luciferin for luciferase assay. (a) *In vitro* luciferase assay with concentrations of luciferin ranging from 0.008 to 8.0 mg/mL. Optimal luminescence was observed at 0.5 mg/mL. (b) *In vivo* luciferase assay in peritoneal dissemination model mice. Luminescence intensity was similar following i.p. injection of 0.5, 1.0, and 1.5 mg luciferin. (c) WST-8 assay showed that cell proliferation was inhibited at luciferin concentrations ≥1.0 mg/mL.

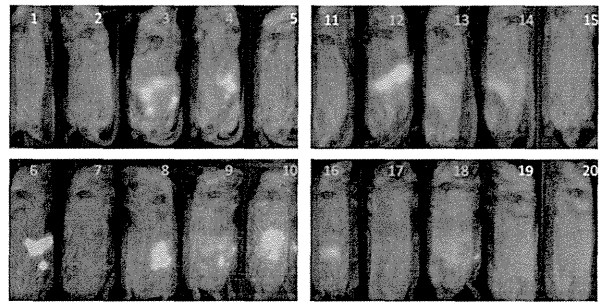

Fig. 2. *In vivo* luciferase assay to evaluate peritoneal dissemination on day 1. Mice were anesthetized with 2–5% isoflurane, and 0.5 mg luciferin was injected i.p. Luciferase assay was carried out within 5 min of injection, and images were captured after 20 min. Luminescence was observed in mouse no. 3, 4, 6, 7, 8, 9, 10, 11, 12, 13, 16, 17, and 18.

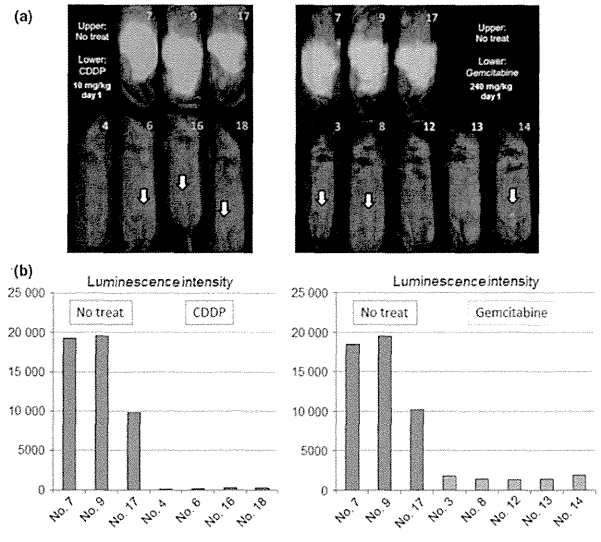

Fig. 3. *In vivo* luciferase assay to evaluate drug efficacy on day 10. (a) Intense luminescence was observed in the no treatment (no treat) group. Mouse no. 10 in this group died on day 9. White arrows show areas of luminescence. In the cisplatin (CDDP) group, luminescence was observed in mouse no. 6, 16, and 18 but not in mouse no. 4. In the gemcitabine group, luminescence was observed in mouse no. 3, 8, and 14. (b) Luminescence intensity was calculated by Image J software. Luminescence intensity was significantly stronger in the no treatment group than that in the CDDP and gemcitabine groups.

three of the four mice in the CDDP group (Fig. 3a), and in three of the five mice in the gemcitabine group. Luminescence intensity in the no treatment group was significantly stronger than that in the CDDP and gemcitabine groups (Fig. 3b).

Evaluation of drug efficacy by *ex vivo* luciferase assay. *Ex vivo* luciferase assay was carried out on day 10 to evaluate the efficacy of i.p. injected anticancer agents. Luminescent spots were observed in all four areas in all three groups (Fig. 4a, Table 1). However, the total number of spots was significantly higher in the no treatment group than that in both the CDDP and gemcitabine groups. On evaluation by area, there were significantly more luminescent spots in the no treatment group

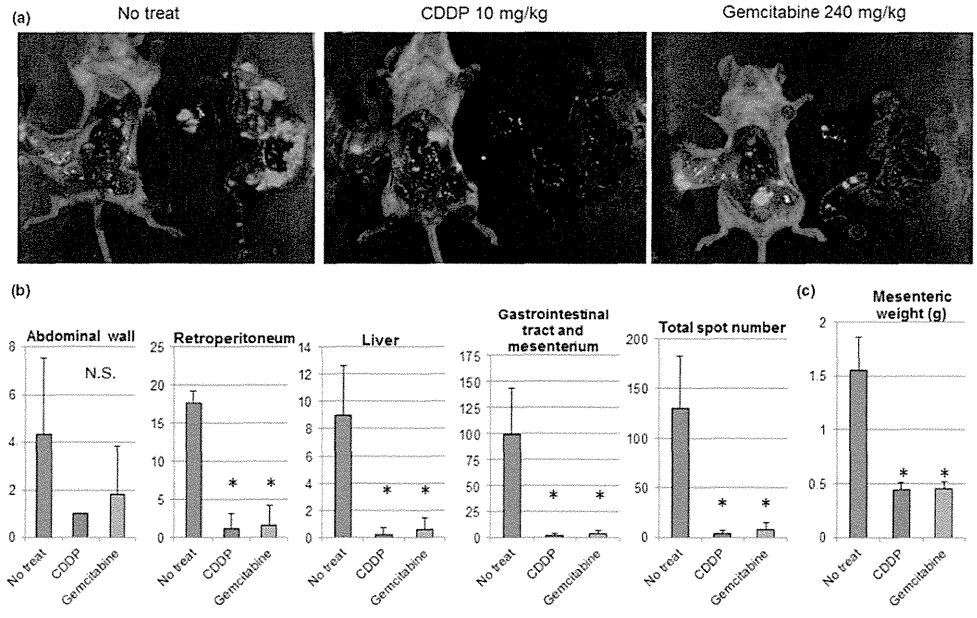

Fig. 4. *Ex vivo* luciferase assay on day 10. (a) Mice were killed under sufficient anesthesia. The abdomen was opened and divided into four areas: the abdominal wall, retroperitoneum, liver, and gastrointestinal tract and mesenterium. Luciferin (1.0 mg) was applied evenly over the four areas. Luminescence was captured for 10 min. Luminescent spots were observed in all areas in all groups. Compared with the no treatment (no treat) group, luminescent spots were reduced in groups treated with cisplatin (CDDP) or gemcitabine. (b) The number of luminescent spots was counted in each area in each group. In groups treated with CDDP or gemcitabine, the total number and the number of luminescent spots in all areas except the abdominal wall area were significantly reduced compared with the no treatment group. (c) Mesenteric weight was significantly heavier in the no treatment group than that in the CDDP and gemcitabine groups. $^*P < 0.05$. N.S., not significant.

Table 1. Number of luminescent spots in each treatment group of mice, by area and in total in *ex vivo* luciferase assay and mesenteric weights, to evaluate peritoneal microdissemination and therapeutic effect

No.	Treatment	Abdominal wall	Retroperitoneum	Liver	Gastrointestinal tract and mesenterium	Total	Mesenteric weight, g
7	No treat	3	18	8	90	119	1.9
9	No treat	8	19	13	147	187	1.44
17	No treat	2	16	6	60	84	1.32
4	CDDP	1	0	0	0	1	0.38
6	CDDP	1	4	0	1	6	0.53
16	CDDP	1	1	1	4	7	0.4
18	CDDP	1	0	0	0	1	0.46
3	Gemcitabine	4	6	2	7	19	0.35
8	Gemcitabine	1	2	1	4	8	0.47
12	Gemcitabine	0	0	0	1	1	0.42
13	Gemcitabine	4	0	0	6	10	0.54
14	Gemcitabine	0	0	0	1	1	0.47

Mice were grouped according to treatment: no treatment (no treat); 10 mg/kg cisplatin (CDDP); and gemcitabine 240 mg/kg.

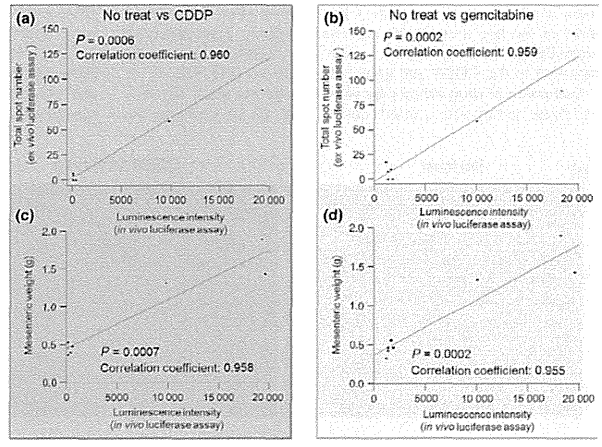

Fig. 5. Positive correlation of luminescence intensity with total luminescent spot number and mesenteric weight. (a, B) In each group, luminescence intensity in in vivo luciferase assay was positively correlated with the total number of luminescent spots in ex vivo luciferase assay. (c, d) In each group, luminescence intensity was positively correlated with mesenteric weight. CDDP, cisplatin; No treat, no treatment.

compared with those in the treatment groups for all areas except the abdominal wall (Fig. 4b). Mesenteric weight was significantly heavier in the no treatment group than that in the treatment groups (Fig. 4c). There was no significant difference in body weight among the three groups at any time point (Fig. S4).

Luminescence intensity positively correlated with total number of luminescent spots and mesenteric weight. In each group, there was a positive correlation between luminescence intensity in *in vivo* luciferase assay and the total number of luminescent spots in *ex vivo* luciferase assay (Fig. 5a,b). Furthermore, there was a positive correlation between luminescence intensity in *in vivo* luciferase assay and mesenteric weight (Fig. 5c,d) and between the total number of luminescent spots in *ex vivo* luciferase assay and mesenteric weight.

Discussion

In this study, we developed a novel peritoneal microdissemination mouse model using luciferase assay. This model has a number of advantages over previously reported mouse models of peritoneal dissemination. First, the optimal luciferin concentration that reduced cell viability was validated for *in vivo* luciferase assay. Second, peritoneal microdissemination could be quantitatively evaluated using *in vivo* luciferase assay. Finally, the model showed a positive correlation between luminescence in *in vivo* luciferase assay and the extent of tumor spread evaluated by *ex vivo* luciferase assay and mesenteric weight.

Previous studies have used 2.0–5.0 mg luciferin i.p. injected for *in vivo* luciferase assay to evaluate tumor extent in the peritoneal cavity.[14–18] Luciferin is thought to have low cytotoxicity for peritoneal tumor clusters analyzed by luciferase assay.[21] However, it remained unclear whether luciferin had a cytotoxic effect on colon 26-luc cells. Therefore, we investigated the optimal concentration and found that the dose of luciferin used in previous studies reduced cell viability in colon 26-luc cells. An i.p. injection of 0.5 mg luciferin was sufficient to produce optimal luminescent intensity.

We focused on the detection of macroscopically invisible peritoneal microdissemination using luciferase assay. The diameter of peritoneally disseminated tumors is usually heterogeneous. Therefore, small clusters of cancer cells might be affected by the cytotoxic effect of the high concentrations of luciferin used in previous models. We believe that the model developed in the present study can more accurately evaluate the efficacy of therapeutic drugs, particularly for peritoneal micrometastasis.

The transplantation rate of colon 26-luc cells by i.p. inoculation was 95% in this study. Although this was sufficient, a rate of 100% is ideal. Experimental bias relating to tumor implantation is one reason why large numbers of experimental animals are needed for *in vivo* studies of anticancer drug efficacy. To address this problem, it is important to identify which experimental animals have successfully been implanted with peritoneal tumors. Therefore, we used the *in vivo* luciferase assay not only to evaluate anticancer drug efficacy but also to identify successfully tumor-implanted mice for the study. *In vivo* luciferase assay before treatment was useful to confirm the engraftment of invisible micrometastasis in a setting where tumor clusters could not be detected by conventional methods, such as macroscopic observation. This strategy resulted in a transplantation rate of 100% in mice that were included in the experiment and provides an effective approach to reduce the number of laboratory animals for drug efficacy assays.

In previous studies, tests of drug efficacy were carried out after day 14.[11,19] We i.p. injected anticancer agents on day 1, and evaluated drug efficacy on day 10 using luciferase assay and mesenteric weight. Therefore, our mouse model reduced the required experimental period with confirmation of tumor engraftment on day 1 and assessment of microdissemination on day 10.

First, we validated the correlation between *in vivo* luciferase activity and peritoneal tumor extent as determined by mesenteric weight and the number of luminescent spots in *ex vivo* luciferase assay. This is very important data to confirm the accuracy and usefulness of experimental mouse models of peritoneal dissemination. However, few previous studies have investigated whether luminescent intensity viewed through the intact abdominal wall could be used to evaluate the extent of peritoneal dissemination. Therefore, our

method to quantitatively evaluate peritoneal dissemination *in vivo* provides an important advance over previous methods using luciferase assay. Incidentally, in *ex vivo* luciferase assay, the number of luminescent spots in the abdominal wall area did not significantly reduce in the treatment group. Based on the luminescence in this area, abdominal wall metastasis may be mixed as well as peritoneal dissemination. Therefore, it was suggested that enough efficacy against abdominal wall metastasis was not provided by i.p. administration of drugs.

Most previous studies have used the *in vivo* imaging system (IVIS) to evaluate luminescence.[14–17] The IVIS system is widely used for *in vivo* imaging by luciferase assay because of its high sensitivity, high throughput, and high resolution. However, this system is expensive for individual laboratories. In this study, we used the lower-priced OptimaShot CL-420α system and a custom-made box for 12 mice. This makes the model applicable to a wide range of experimental settings.

In summary, we established a novel method to evaluate tumorigenesis and drug efficacy using a mouse model of peritoneal microdissemination and luciferase assay. New drugs and treatment protocols to treat local dissemination will improve outcomes in patients with tumors in the peritoneal cavity. This model is useful to validate peritoneal micrometastasis formation and to evaluate drug efficacy with high accuracy, reduced experimental costs, and reduced the need to kill experimental animals.

Acknowledgments

The authors thank Tamami Higuchi and Mariko Nakamura for their assistance. We also thank the staff at the Bioresource Center, Gunma University Graduate School of Medicine for technical help with the animal experiments. This work was supported in part by the Uehara Memorial Foundation, the Promotion Plan for the Platform of Human Resource Development for Cancer, and the Japan Society for the Promotion of Science Grant-in Aid for Scientific Research (15K10085 and 22591450).

Disclosure Statement

The authors have no conflict of interest.

References

1 Coccolini F, Gheza F, Lotti M *et al.* Peritoneal carcinomatosis. *World J Gastroenterol* 2013; **19**: 6979–94.
2 Shimizu T, Sonoda H, Murata S *et al.* Hyperthermic intraperitoneal chemotherapy using a combination of mitomycin C,5-fluorouracil, and oxaliplatin in patients at high risk of colorectal peritoneal metastasis: a Phase I clinical study. *Eur J Surg Oncol* 2014; **40**: 521–8.
3 Levine EA, Stewart JH 4th, Shen P, Russell GB, Loggie BL, Votanopoulos KI. Intraperitoneal chemotherapy for peritoneal surface malignancy: experience with 1,000 patients. *J Am Coll Surg* 2014; **218**: 573–85.
4 Ishigami H, Kitayama J, Kaisaki S *et al.* Phase II study of weekly intravenous and intraperitoneal paclitaxel combined with S-1 for advanced gastric cancer with peritoneal metastasis. *Ann Oncol* 2010; **21**: 67–70.
5 Aletti GD, Dowdy SC, Gostout BS *et al.* Aggressive surgical effort and improved survival in advanced-stage ovarian cancer. *Obstet Gynecol* 2006; **107**: 77–85.
6 Armstrong DK, Bundy B, Wenzel L *et al.* Intraperitoneal cisplatin and paclitaxel in ovarian cancer. *N Engl J Med* 2006; **354**: 34–43.
7 Sugarbaker PH. Update on the prevention of local recurrence and peritoneal metastases in patients with colorectal cancer. *World J Gastroenterol* 2014; **20**: 9286–91.
8 Archer S, Gray B. Intraperitoneal 5-fluorouracil infusion for treatment of both peritoneal and liver micrometastases. *Surgery* 1990; **108**: 502–7.
9 Fujimoto S, Shrestha RD, Kokubun M *et al.* Intraperitoneal hyperthermic perfusion combined with surgery effective for gastric cancer patients with peritoneal seeding. *Ann Surg* 1988; **208**: 36–41.
10 Yan TD, Cao CQ, Munkholm-Larsen S. A pharmacological review on intraperitoneal chemotherapy for peritoneal malignancy. *World J Gastrointest Oncol* 2010; **2**: 109–16.
11 Hashimoto S, Yazawa S, Asao T *et al.* Novel sugar-cholestanols as anticancer agents against peritoneal dissemination of tumor cells. *Glycoconj J* 2008; **25**: 531–44.
12 Haruki K, Shiba H, Fujiwara Y *et al.* Inhibition of nuclear factor-κB enhances the antitumor effect of paclitaxel against gastric cancer with peritoneal dissemination in mice. *Dig Dis Sci* 2013; **58**: 123–31.
13 Yamada J, Kitayama J, Tsuno NH *et al.* Intra-peritoneal administration of paclitaxel with non-animal stabilized hyaluronic acid as a vehicle–a new strategy against peritoneal dissemination of gastric cancer. *Cancer Lett* 2008; **272**: 307–15.
14 Toyoshima M, Tanaka Y, Matumoto M *et al.* Generation of a syngeneic mouse model to study the intraperitoneal dissemination of ovarian cancer with *in vivo* luciferase imaging. *Luminescence* 2009; **24**: 324–31.
15 Yang SW, Chanda D, Cody JJ *et al.* Conditionally replicating adenovirus expressing TIMP2 increases survival in a mouse model of disseminated ovarian cancer. *PLoS ONE* 2011; **6**: e25131.
16 Lan KL, Ou-Yang F, Yen SH, Shih HL, Lan KH. Cationic liposome coupled endostatin gene for treatment of peritoneal colon cancer. *Clin Exp Metastasis* 2010; **27**: 307–18.
17 Haley ES, Au GG, Carlton BR, Barry RD, Shafren DR. Regional administration of oncolytic Echovirus 1 as a novel therapy for the peritoneal dissemination of gastric cancer. *J Mol Med* 2009; **87**: 385–99.
18 Hyoudou K, Nishikawa M, Ikemura M *et al.* Cationized catarase-loaded hydrogel for growth inhibition of peritoneal disseminated tumor cells. *J Control Release* 2007; **122**: 151–8.
19 Okamura A, Yazawa S, Nishimura T *et al.* A new method for assaying adhesion of cancer cells to the greater omentum and its application for evaluating anti-adhesion activities of chemically synthesized oligosaccharides. *Clin Exp Metastasis* 2000; **18**: 37–43.
20 Asao T, Yazawa S, Kudo S, Takenoshita S, Nagamachi Y. A novel *ex vivo* method for assaying adhesion of cancer cells to the peritoneum. *Cancer Lett* 1994; **78**: 57–62.
21 Tiffen JC, Bailey CG, Ng C, Rasko JE, Holst J. Luciferase expression and bioluminescence does not affect tumor cell growth *in vitro* or *in vivo*. *Mol Cancer* 2010; **9**: 299.

Supporting Information

Additional supporting information may be found in the online version of this article:

Fig. S1. Custom-made box used for luciferase assay.

Fig. S2. Assessment of *ex vivo* luciferase assay in each organ area: the abdominal wall, retroperitoneum, liver, and gastrointestinal tract and mesenterium.

Fig. S3. *In vivo* luciferase assay on day 10 in mice with no luminescence on day 1.

Fig. S4. Body weight change among the three groups.

J Hepatobiliary Pancreat Sci (2016) ••:••–••
DOI: 10.1002/jhbp.345

ORIGINAL ARTICLE

Impact of human T-cell leukemia virus type 1 on living donor liver transplantation: a multi-center study in Japan

Tomoharu Yoshizumi · Yasutsugu Takada · Ken Shirabe · Toshimi Kaido · Masaaki Hidaka · Masaki Honda · Takashi Ito · Masahiro Shinoda · Hideki Ohdan · Naoki Kawagishi · Yasuhiko Sugawara · Yasuhiro Ogura · Mureo Kasahara · Shoji Kubo · Akinobu Taketomi · Natsumi Yamashita · Shinji Uemoto · Hiroki Yamaue · Masaru Miyazaki · Tadahiro Takada · Yoshihiko Maehara

The author's affiliations are listed in the Appendix.

Correspondence to: Tomoharu Yoshizumi, Department of Surgery and Science, Graduate School of Medical Sciences, Kyushu University, 3-1-1 Maidashi, Fukuoka 812-8582, Japan.
e-mail: yosizumi@surg2.med.kyushu-u.ac.jp

DOI: 10.1002/jhbp.345

Abstract

Background The natural history of human T-cell leukemia virus type 1 (HTLV-1), which causes adult T-cell leukemia (ATL) or HTLV-1 associated myelopathy, after liver transplantation is unclear.

Methods We conducted a nationwide survey to investigate the impact of HTLV-1 status on living donor liver transplantation (LDLT) in Japan. We analyzed the cases of 82 HTLV-1-positive recipients and six HTLV-1-negative-before-LDLT recipients who received a hepatic graft from HTLV-1-positive donors.

Results Adult T-cell leukemia developed in five recipients who ultimately died. Of these five, two received grafts from HTLV-1-positive donors and three from HTLV-1-negative donors. The 1-, 3-, and 5-year ATL development rates were 4.5%, 6.5%, and 9.2%, respectively. Fulminant hepatic failure as a pre-transplant diagnosis was identified as an independent risk factor for ATL development ($P = 0.001$). The 1-, 3-, and 5-year survival rates for HTLV-1-positive recipients who received grafts from HTLV-1-negative donors were 79.9%, 66.1%, and 66.1%, and from HTLV-1-positive donors were 83.3%, 83.3%, and 60.8%, respectively. The 1-year survival rate for HTLV-1-negative recipients who received grafts from HTLV-1-positive donors was 33.3%.

Conclusions Fulminant hepatic failure is an independent risk factor for ATL development in HTLV-1-positive recipients. Grafts from HTLV-1-positive living donors can be transplanted into selected patients.

Keywords Adult T-cell leukemia · Human T-cell leukemia virus type 1 · Living donor liver transplantation

Introduction

Human T-cell leukemia virus type 1 (HTLV-1) is a retrovirus that is endemic in southwestern Japan and causes adult T-cell leukemia (ATL) or HTLV-1 associated myelopathy (HAM) in a minority of carriers, although most carriers remain asymptomatic. HTLV-1-infected recipients who are concurrently treated with immunosuppressive drugs following organ or bone marrow transplantations might exhibit an accelerated or altered developmental course of HTLV-1-associated diseases [1]. We previously reported on the impact of HTLV-1 status in living donor liver transplantation (LDLT) as a single-center experience [2, 3]. From that study, we concluded that pre-transplant fulminant hepatic failure (FHF) is a risk factor for ATL development in HTLV-1-positive recipients [2]. HTLV-1 is vertically transmitted from mothers to infants, and the virus is maintained within the infant's family [4]. In Japan, living

donors are limited to the blood relatives or spouse of the intended recipient, except in very rare cases. Therefore, sometimes both the donor candidate and the recipient are HTLV-1 positive.

Approximately 1.1 million individuals in Japan are infected with HTLV-1 [5], and 30% of HTLV-1 carriers live in southwestern Japan. The Japan Organ Transplant Network recommends against using organs from HTLV-1-positive donors even for recipients with a pre-existing HTLV-1 infection. In contrast, most transplant centers do accept HTLV-1-positive carriers as living donors. There is a widening gap between the need for livers and the availability of livers donated by deceased individuals in most countries. The use of HTLV-1-positive donors is increasing owing to the growing disparity between organ availability and demand [6]. There are many recipients with an urgent need for transplant, especially older individuals, and, to fill this demand, livers from HTLV-1-positive donors could be considered for use in recipients who are already HTLV-1 positive.

Because Japan is located in an HTLV-1 endemic area, we collected data to report the nationwide figures on HTLV-1-positive donors or recipients who underwent LDLT. Our data show HTLV-1 transmission in a liver transplantation (LT) setting and provide important information for transplant surgeons performing LT with HTLV-1 positive donors or recipients.

Patients and methods

Recipients

As a retrospective survey, we analyzed the cases of 82 recipients who were HTLV-1 positive before LDLT and of six recipients who were HTLV-1 negative before LDLT, all of whom received hepatic grafts from HTLV-1-positive donors. These recipients underwent LDLT at the following 13 institutions prior to or during October 2014: Kyushu University (32 recipients), Kyoto University (19 recipients), Nagasaki University (12 recipients), Kumamoto University (12 recipients), Kyoto Prefectural University of Medicine (two recipients), Keio University (two recipients), Tohoku University (two recipients), Hiroshima University (two recipients), Ehime University (one recipient), National Center for Child Health and Development (one recipient), Nagoya University (one recipient), The University of Tokyo (one recipient), and Osaka City University (one recipient). This study was conducted in collaboration with the Japanese Society of Hepato-Biliary-Pancreatic Surgery and the Japanese Liver Transplantation Society. The institutional review boards of each institution approved this study (Representative Institution; Kyushu University 25–298). The primary diagnoses requiring LDLT for the 82 HTLV-1-positive recipients were as follows: hepatitis C virus (HCV) in 33 recipients (19 had hepatocellular carcinoma, HCC), FHF in 12 recipients, primary biliary cirrhosis in seven recipients (one had HCC), biliary atresia in seven recipients, cryptogenic in six recipients (one had HCC), hepatitis B virus (HBV) in three recipients (one had HCC), autoimmune hepatitis in three recipients (one had HCC), primary sclerosing cholangitis in two recipients, and HBV + HCV with HCC, secondary biliary cirrhosis, idiopathic portal hypertension with cholangiocellular carcinoma, alcohol abuse, nonalcoholic steatohepatitis, polycystic liver disease, extrahepatic portal stenosis, graft failure, and chronic rejection in one recipient each (Table 1). The primary diagnoses requiring LDLT for the six HTLV-1-negative recipients transplanted with grafts from HTLV-1-positive donors were as follows: alcohol abuse in three, HCV in two, and FHF in one recipient(s) (Table 2).

Donors

Donors were selected from candidates who volunteered to be living donors. The donors for the HTLV-1-positive recipients were children in 39, siblings in 15, spouses in 13, parents in eight, uncles in two, siblings-in-law in two, a daughter-in-law in one, a niece in one, and a domino transplant in one case(s). The HTLV-1-positive donors for the HTLV-1-negative recipients were siblings in three, spouses in two, and a father in one case(s) (Table 2).

Graft type

The selection of graft type depended on the criteria for each institution. The graft types for the HTLV-1-positive recipients were right lobe in 36, extended left lobe in 21, left lobe in 13, right posterior sector in four, left lateral segment in two, dual graft in one, domino whole liver graft in one, and reduced S2 graft in one case(s). The graft types from the HTLV-1-positive donors for the HTLV-1-negative recipients were right lobe in five and extended left lobe with caudate lobe in one case(s).

Splenectomy

Simultaneous splenectomy during LDLT was performed under the criteria of each institution. This procedure was typically performed to decrease portal pressure or to improve pancytopenia.

Table 1 Characteristics of human T-cell leukemia virus type 1 (HTLV-1)-positive recipients at living donor liver transplantation (LDLT)

Variables	Cases (n = 82)
Recipient age (years, range)	50.2 (4 months–74 years)
Recipient gender (male, %)	37 (45.1)
Primary diagnosis	
Liver cirrhosis	
Hepatitis C/Hepatitis B/Hepatitis B + C	33/3/1
Cryptogenic/Alcohol/NASH/AIH	6/1/1/3
Fulminant hepatic failure	12
Cholestatic disease: PBC/BA/PSC/Secondary biliary cirrhosis	7/7/2/1
Others[a]	4
Recipient height (cm, range)	157 (60–183)
Recipient weight (kg)	58 (5.4–94)
MELD score (range)	19.0 (4–42)
Splenectomy (yes, %)	36 (45.6)[b]
Recipient operation time (min, range)	816 (437–1407)
Recipient blood loss (ml, range)	7934 (217–60860)
Calcineurin inhibitor (tacrolimus, %)	67 (81.7)
MMF or mizoribine (yes, %)	46 (56.1)
Donor HTLV-1 positive (yes, %)	12 (15.0)[c]
Graft (right, %)	36 (43.9)
GW/SLW ratio (%, range)	47.5 (23.6–131.5)
GW-BW ratio (%, range)	0.96 (0.44–4.97)
ABO (identical/compatible/incompatible)	49/24/9
Blood relative donor (yes, %)	64 (78.0)
Donor age (years, range)	39.7 (18–65)
Donor gender (male, %)	45 (55.5)[d]
Donor operation time (min, range)	437 (226–738)
Donor blood loss (ml, range)	541 (70–3500)

AIH autoimmune hepatitis, *BA* biliary atresia, *BW* body weight, *GW* graft weight, *MELD* model for end-stage liver disease, *NASH* non-alcoholic steatohepatitis, *PBC* primary biliary cirrhosis, *PSC* primary sclerosing cholangitis, *SLW* standard liver weight calculated by 706.2 × body surface area + 2.4

[a] Others included polycystic liver disease, extrahepatic portal stenosis, graft failure and chronic rejection

[b] Unknown in three recipients

[c] HTLV-1 status was unknown in two donors

[d] One patient got dual grafts from two donors

Immunosuppression regimen

Initial immunosuppression was started with either tacrolimus or cyclosporine A in combination with steroid and/or mycophenolate mofetil (MMF) or mizoribine. For the HTLV-1-positive recipients, tacrolimus was used in 67 recipients, and cyclosporine A in 14 recipients. A calcineurin inhibitor was used in all but one recipient. Steroids were used in 77 recipients. MMF was used in 44 recipients, and mizoribine in two recipients. An anti-IL-2 receptor antibody was used in 13 recipients, and rituximab was used in five recipients. For HTLV-1-negative recipients who received HTLV-1-positive grafts, tacrolimus was used in five recipients, and cyclosporine A in one recipient. Steroids were used in all but one recipient, mizoribine was used in one recipient, and antibodies were not used in any recipients (Table 2).

Follow-up

The mean follow-up period was 1,643 days, with 360 days and 2,897 days as the 25th and 75th percentiles, respectively. Recipient survival was defined as the time period between LDLT and recipient death.

Statistical analyses

Recipient survival rates and ATL development rates were calculated by the Kaplan–Meier product-limited method. Information about the recipients was collected on their day of death when a recipient died from a disease other than ATL to calculate the ATL development rate. Variables that were included in the univariate analysis by a Fisher's exact test were recipient age, donor age, etiology of liver disease, donor HTLV-1 status, splenectomy, graft weight (GW)-standard liver weight (SLW) ratio, graft type, model for end-stage liver disease (MELD) score, recipient sex, donor sex, blood type compatibility, presence of blood relative between donor and recipient, tacrolimus or cyclosporine A use, and MMF use. For the multivariate analysis, an exact logistic regression analysis was performed. Data are expressed as means ± standard deviation. All statistical analyses were performed using JMP 11.0 software (SAS, Inc., Cary, NC, USA). A P-value of <0.05 is considered significant.

Results

There were 37 male and 45 female HTLV-1-positive recipients, and their mean age was 50.2 years (range: 4 months–74 years). Their mean MELD score was 19.0 (range: 4–42), and their mean GW-SLW ratio was 47.5 (range: 23.6–131.5). Their mean GW-recipient body weight ratio was 0.96 (range: 0.44–4.97). Forty-five donors were male and 36 were female, and they had a mean age of 39.7 years (range: 18–65). One recipient was transplanted with dual grafts from male and female donors. Sixty-four (78.0%) donors were blood relatives with their recipients. Twelve of the 82 donors were HTLV-1 positive. The clinical courses of these 12 donors were uneventful after hepatectomy. No donors developed ATL or HAM after the surgery.

Table 2 Characteristics of human T-cell leukemia virus type 1 (HTLV-1) negative recipients who received grafts from HTLV-1 positive donors and their outcome after living donor liver transplantation (LDLT)

Variables	1	2	3	4	5	6
Recipient age	41	44	57	48	15	59
Recipient gender	M	M	F	M	F	M
Diagnosis	Alcohol	LC-C	Alcohol	LC-C	FHF	Alcohol
MELD	11	19	25	23	28	NA
Splenectomy	No	Yes	No	NA	No	NA
Initial CNI	TAC	TAC	TAC	CYA	TAC	TAC
Steroid	Yes	Yes	Yes	Yes	Yes	No
MMF or mizoribine	No	No	No	Mizoribine	No	No
Donor age	43	39	55	44	49	55
Donor gender	F	F	F	M	M	F
Graft	RL	RL	RL	LL + C	RL	RL
GW-SLW (%)	44.8	50.0	56.7	37.7	63.4	41.6
GW-BW (%)	0.76	1.01	1.11	0.75	1.34	0.83
ABO	Compatible	Identical	Identical	Identical	Identical	Identical
Relation to recipient	Sibling	Spouse	Sibling	Sibling	Father	Spouse
ATL	No	No	No	No	No	No
HAM	No	No	No	No	No	No
Survival time (days)	3457	59	19	22	3612	26
Alive	Alive	No	No	No	Alive[a]	No
Cause of death	–	Heart failure	Graft infarction	Graft infarction	–	Cerebral hemorrhage

ATL adult T-cell leukemia, *CYA* cyclosporine A, *FHF* fulminant hepatic failure, *GW* graft weight, *HAM* HTLV-1 associated myelopathy, *LC-C* liver cirrhosis type C, *LL + C* extended left lobe with caudate lobe graft, *RL* right lobe graft, *SLW* standard liver weight, *TAC* tacrolimus

[a] Patient #5 underwent a re-transplantation due to chronic rejection

The HTLV-1 statuses of two of the donors were unknown. The characteristics of the HTLV-1-positive recipients and their donors at LDLT are shown in Table 1.

Adult T-cell leukemia developed in five recipients (Table 3). The intervals between LDLT and ATL development for these five recipients were 181 days, 291 days, 257 days, 823 days, and 1,315 days. Two of the ATL recipients received grafts from HTLV-1 carriers and three received them from non-carriers (Table 3). Fluorescent *in situ* hybridization revealed that the development of ATL in two of the recipients was owing to the recipient having HTLV-1 [2].

The 1-, 3-, and 5-year ATL development rates in the HTLV-1-positive recipients were 4.5%, 6.5%, and 9.2%, respectively (Fig. 1). Four recipients died despite chemotherapy owing to ATL. One recipient with ATL died of chronic rejection owing to the withdrawal of treatment with a calcineurin inhibitor [2]. The intervals between ATL development and recipient death for these five recipients were 15 days, 3 months, 5 months, 15 months, and 27 months. The overall survival rate based on recipient and donor HTLV-1 status is shown in Figure 1. The 1-, 3-, 5-, and 10-year survival rates for HTLV-1-positive recipients who received grafts from HTLV-1-negative donors were 79.9%, 66.1%, 66.1%, and 59.7%, respectively. The causes of death that were unrelated to ATL were sepsis in 10, HCC recurrence in four, graft failure in four, graft infarction in one, and CCC recurrence in one recipient(s). We were unable to obtain follow-up data for one recipient. In contrast, the 1-, 3-, 5-, and 10-year survival rates for the HTLV-1-positive recipients who received grafts from HTLV-1-positive donors were 83.3%, 83.3%, 60.8%, and 48.6%, respectively. The three recipients whose deaths were unrelated to ATL died from post-transplant lymphoproliferative disorder (PTLD) in the brain, heart failure, and suicide (one recipient each).

Six HTLV-1-negative recipients received grafts from HTLV-1-positive donors (Table 2). Four of these six recipients died within 2 months after LDLT. Therefore, the 1-year survival rate after LDLT for these patients was 33.3% (Fig. 1). Their causes of death were graft infarction in two recipients, heart failure in one recipient, and cerebral hemorrhage in one recipient. Furthermore, one recipient underwent re-transplantation because of chronic rejection (Table 2).

Univariate analyses revealed that, in this study, both FHF as a pre-transplant diagnosis and a lack of splenectomy were risk factors for ATL development ($P < 0.001$ and $P = 0.013$, respectively; Table 4). Other factors, including donor HTLV-1 status, were not found to be

Table 3 Characteristics and outcome of recipients who developed adult T-cell leukemia (ATL) after living donor liver transplantation (LDLT)

Variables	1	2	3	4	5
Recipient age at LDLT	39	45	67	48	59
Recipient gender	F	M	M	M	F
Recipient HTLV-1	Positive	Positive	Positive	Positive	Positive
Diagnosis	FHF	FHF	FHF	FHF	FHF
MELD	23	22	22	25	32
Splenectomy	No	No	No	No	No
Initial CNI	TAC	TAC	TAC	CYA	TAC
Steroid	Yes	Yes	Yes	Yes	Yes
MMF or mizoribine	No	No	No	No	No
Donor age at LDLT	46	56	34	20	28
Donor gender	M	F	M	M	F
Donor HTLV-1	Positive	Positive	Negative	Negative	Negative
Graft	LL	LL	RL	RL	RL
GW-SLW (%)	35.1	42.6	54.9	50.2	37.6
GW-BW (%)	0.64	0.89	1.00	0.89	0.79
ABO	Identical	Compatible	Compatible	Identical	Identical
Relation to recipient	Sibling	Sibling	Son	Son	Daughter
HAM	No	No	No	No	No
Survival time (days)	195	1273	432	2107	360
Alive	No	No	No	No	No
Cause of death	ATL	Chronic rejection	ATL	ATL	ATL

CYA cyclosporine A, *FHF* fulminant hepatic failure, *GW* graft weight, *HAM* HTLV-1 associated myelopathy, *LL* left lobe graft, *RL* right lobe graft, *SLW* standard liver weight, *TAC* tacrolimus

risks for ATL development. A multivariate analysis revealed that FHF was an independent risk factor for ATL development (P = 0.001, Table 5).

HTLV-1 associated myelopathy developed in two recipients, and both were HTLV-1 positive before LDLT. The primary diagnosis for both of these two recipients was HCV. The donor was HTLV-1-positive for one of these two recipients [7]. A simultaneous splenectomy was performed in one recipient. The intervals between LDLT and HAM development for these two patients were 15 months and 46 months. One recipient died because of chronic rejection 8 months after HAM development, and the other was still alive 101 months after HAM development.

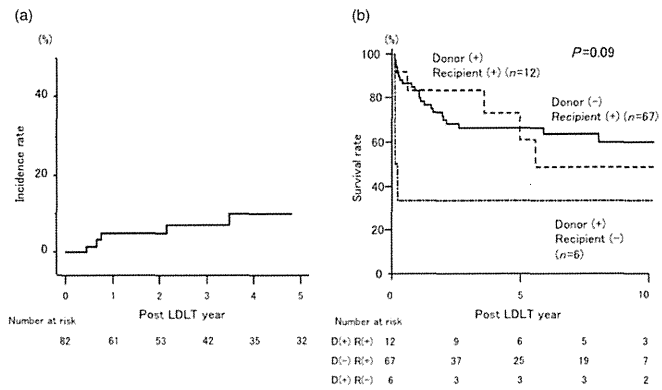

Fig. 1 Adult T-cell leukemia (ATL) development rate and survival after living donor liver transplantation (LDLT). Eighty-eight recipients underwent LDLT. (**a**) The ATL development rate in 82 human T-cell leukemia virus type 1 (HTLV-1)-positive recipients. (**b**) The overall recipient survival after LDLT. The HTLV-1 status was unknown in two of the donors. Follow-up data for one of the HTLV-1-positive recipients who received a graft from an HTLV-1-negative donor were not obtained